Title

Atmospheric CO_2 measurements and error analysis on seasonal air–sea CO_2 fluxes in the Bay of Biscay.

Authors

Padin, X.A.[1], Vázquez-Rodríguez, M.[1], Rios, A.F.[1] and Pérez, F.F.[1]

[1] Instituto de Investigacións Mariñas (CSIC). Eduardo Cabello 6, 36208 Vigo, Spain

Corresponding author

Ríos, A.F.

Instituto de Investigacións Mariñas (CSIC). Eduardo Cabello 6, 36208 Vigo, Spain

Telf. +34-986-231930 (Ext. 371)

Fax. +34-986-292762

E-mail: aida@iim.csic.es

Keywords

Carbon dioxide; air-sea exchanges; seasonal variations; Bay of Biscay; ships of opportunity

ABSTRACT

Atmospheric molar fraction of CO_2 (xCO_2^{atm}) measurements obtained on board of ships of opportunity are used to parameterize the seasonal cycle of atmospheric xCO_2 (xCO_2^{atm}) in three regions of the Eastern North Atlantic (Galician and French offshore and Bay of Biscay). Three selection criteria are established to eliminate spurious values and identify xCO_2^{atm} data representative of atmospheric background values. The filtered dataset is fitted to seasonal curve, consisting of an annual trend plus a seasonal cycle. Although the fitted curves are consistent with the seasonal evolution of xCO_2^{atm} data series from land meteorological stations, only ship-board measurements can report the presence of winter xCO_2^{atm} minimum on Bay of Biscay. Weekly air-sea CO_2 flux differences (mmolC·m^{-2}·day^{-1}) produced by the several options of xCO_2^{atm} usually used (ship-board measurements, data from land meteorological stations and annually averaged values), were calculated in Bay of Biscay throughout 2003. Flux error using fitted seasonal curve relative to on board measurements was minimal whereas land stations and annual means yielded random (-0.2 ± 0.3 mmolC·m^{-2}·day^{-1}) and systematic (-0.1 ± 0.4 mmolC·m^{-2}·day^{-1}), respectively. The effect of different available sources of sea level pressure, wind speed and transfer velocity were also evaluated. Wind speed and transfer velocity parameters are found as the most critical choice in the estimate of CO_2 fluxes reaching a flux uncertainty of 7 mmolC·m^{-2}·day^{-1} during springtime. The atmospheric pressure shows a notable relative effect during summertime although its influence is quantitatively slight on annual scale (0.3 ± 0.2 mmolC·m^{-2}·day^{-1}). All results confirms the role of the Bay of Biscay as CO_2 sink for the 2003 with an annual mean CO_2 flux around -5 ± 5 mmolC m^{-2} day^{-1}.

1. INTRODUCTION

The seasonal cycle of the molar fraction of atmospheric CO_2 (xCO_2^{atm}) is the result of a combination of uptake and release of CO_2 by growing plants and soils, seasonal uptake by oceanic waters, and anthropogenic emissions. Although roughly half of the anthropogenic CO_2 is stored to the atmosphere, the xCO_2^{atm} does not seem to be a critical variable in the error estimation of the annual average CO_2 flux. This is because high atmospheric mixing rates keep the seasonal variability of xCO_2^{atm} smaller than that for the seawater molar fraction of CO_2 (xCO_2^{sw}). However, it is important to consider the different sources xCO_2^{atm} data and to evaluate their reliability at annual scale and other temporal scales.

In numerous air-sea CO_2 exchange studies, xCO_2^{atm} was often assumed as constant (Kempe and Pegler 1991; Lefèvre et al. 1998, 1999; Boehm and Grant, 1998; Lefèvre and Moore, 2000; DeGrandpre et al. 1998, 2002; Jabaud-Jan et al. 2004) or obtained from various monitoring land stations (Boden et al., 1991; Conway et al., 1994). Nowadays, a cooperative air sampling network around the world managed and operated by NOAA Earth System Research Laboratory (ESRL) Global Monitoring Division (GMD) is a real alternative to on ship-board xCO_2^{atm} measurements. The data set, available from *http://www.cmdl.noaa.gov/ccgg/flask.html*, represents a practical tool to calculate the net flux of CO_2 through the air-sea interface (*e.g.* Stephens et al. 1995; Hood et al. 1999; Borges and Frankignoulle, 2002; Olsen et al. 2004).

From high frequency data measured on ships of opportunity during 2003 and 2004, the seasonal cycle of xCO_2^{atm} in the Bay of Biscay is compared to time series data from nearby land meteorological stations. Additionally, the air-sea CO_2 flux error associated with the different estimates of xCO_2^{atm} is studied from real data sets throughout the 2003 annual cycle. Finally, the effect of using different estimates of atmospheric pressure, wind speed, and different expressions of transfer velocity, is also explored in order to determine the uncertainty in CO_2 flux on the seasonal scale.

2. MATERIALS AND METHODS

2.1 Data acquisition

The database was obtained using ships of opportunity (RO-RO "L'Audace" and "Surprise") of Suardiaz Company that regularly covered the route Vigo, Spain – St. Nazaire, France (Fig. 1). A total of 116 journeys was performed. Seawater molar fractions of CO_2, and surface values of salinity and temperature were averaged and recorded every minute throughout each transit. Atmospheric molar fraction of CO_2 was as detailed in 2.2 below.

The xCO_2 was measured with a non-dispersive infrared gas analyser (Licor®, LI-6262). At the beginning and the end of each transit (which takes 26 hours), the equipment was calibrated with two standards, CO_2-free air and high CO_2 standard gas with a certified concentration of 375 ppmv (Instituto Meteorológico Nacional, Izaña, Canary Islands). The xCO_2^{sw} in dry air was converted into CO_2 fugacity (fCO_2^{sw}) as described in DOE Handbook (1994). Temperature shift was corrected using the empirical equation proposed by Takahashi et al. (1993). The temperature difference between the ship's sea inlet and the equilibrator was usually under 1ºC.

Water vapor pressure (pH_2O, in atm) was calculated from in situ temperature (T_{is}, in ºC) according to Cooper et al. (1998) to convert the xCO_2^{atm} into fCO_2^{atm}. Following Olsen et al. (2003), a decrease of 0.3% from pCO_2^{atm} to fCO_2^{atm} (Weiss 1974) was considered accurate enough.

$$pCO_2^{atm} = xCO_2^{atm} \cdot (p_{atm} - pH_2O) \quad (1)$$

$$pH_2O = 0.981 \cdot \exp(14.32602 - (5306.83/(273.15 + T_{is})))$$

The exchange of carbon between the atmosphere and the ocean, F (mmol m^{-2} day^{-1}) was calculated using the following equation:

$$F = 0.24\, k\, S\, (fCO_2^{sw} - fCO_2^{atm}) \quad (2)$$

For the computation of CO_2 fluxes (Eq. 2), weekly mean air-sea CO_2 gas transfer velocity, k ($cm \cdot h^{-1}$), were computed according to the three different parameterizations of Liss and Merlivat (1986), Wanninkhof (1992) and Nightingale et al. (2000). The wind speed to estimate the transfer velocity was obtained from two websites. The 6-hourly wind vector product was facilitated by the NCEP/NCAR reanalysis project (Kalnay et al., 1996) from the web site of the NOAA-CIRES Climate Diagnostics Center, Boulder, Co, USA (http://www.cdc.noaa.gov/) and the wind speed measured remotely by the QuikScat satellite was collected from the Physical Oceanography Distributed Active Archive Center of the Jet Propulsion Laboratory (http://podaac.jpl.nasa.gov). Seawater CO_2 solubility (S, mol L^{-1} atm^{-1}) was calculated from Weiss (1974), and the constant 0.24 is a unit conversion factor.

2.2 Atmospheric data treatment

xCO_2^{atm} was measured twenty times in a 5 minutes period each hour during the 2003 and 2004 transits. The raw xCO_2^{atm} data (Fig. 2a) showed a wide variability due to the characteristic ship emissions that increased the natural xCO_2^{atm} range up to 465 ppmv. On other occasions, the difficult working conditions on board and other logistic issues caused long periods (Fig. 2a) without measurements, mainly during the second year. For detailed analysis of trend and variation of xCO_2^{atm}, several quality control criteria were applied to the in situ measurements prior to curve fitting. Three zones were selected along the track: Galician offshore (42.75º–43.25 ºN), Bay of Biscay (44.5º–45.5 ºN) and French offshore (46.15º–46.50 ºN) in order to recognize regional characteristics (Fig. 1).

2.2.1 Data selection

With the aim of eliminate the frequent ship-board contaminations and identifying the representative xCO_2^{atm} values of well-mixed air, three known conditions were utilized for data selection:

1. Data for every five minute periods was averaged and values whose standard deviation exceeded 0.33 ppmv were automatically discarded. This data filter is inspired by Conway et al. (1994) who accepted only paired-samples displaying xCO_2^{atm} differences smaller than 0.5 ppmv. The range of the accepted xCO_2^{atm} data decreased significantly with regard to the raw data (Fig. 2b, black points).

2. The difference between consecutive hourly mean of xCO_2^{atm} in well mixed air is expected to be smaller than 0.25 ppmv (Peterson et al. 1986; Gillete et al. 1987). Due to the continuous change in sampling positions, the acceptable

xCO_2^{atm} difference is widened to be 0.50 ppmv in the hourly-spaced measurements.

3. Following Komhyr et al. (1985), the xCO_2^{atm} measurements obtained at wind speeds monitored at the atmospheric air inlet to the ship's funnel, lower than 2 $m{\cdot}s^{-1}$ were rejected. This third filter eliminated the values possibly affected by local CO_2 sources. Once the second and third criteria were implemented on database already filtered in accordance with criterion (1), values ranged from 360 to 380 ppmv (Fig. 2b, open circles).

The results of the quality control criteria retain different percentages of original data depending on the region of our track. The Galician offshore, Bay of Biscay and French offshore have 80, 50 and 40 % of accepted raw data, respectively. The proportion of retained measurements was analyzed with regard to whether the origin of the air mass was oceanic or terrestrial (Fig. 1). In the three areas of study, the data selection criteria produced a significant increase of measurements performed with oceanic backtrajectory (Bousquet et al. 1996). Therefore, the continental fingerprint related to anthropogenic CO_2 sources could be detected over the Bay of Biscay. Due to the nearness of the coastline, French offshore displayed a significant reduction of xCO_2^{atm} recorded from air masses of terrestrial origin in the filtered xCO_2^{atm}, namely, from 73 to 57%.

2.2.2 Curve fitting

The filtered xCO_2^{atm} values were fitted to a theoretical curve by means of the least squares method. These curves are a combination of terms according to Pérez et al. (2001): a trend and a seasonal cycle with the annual and seasonal harmonics (Thoning et al., 1989).

$$xCO_2^{atm} = a + b \cdot t/365.25 + A_a \cdot \sin(2\pi/365.25 \cdot (t - \theta_a)) + $$
$$+ A_s \cdot \sin(4\pi/365.25 \cdot (t - \theta_s)) \quad (3)$$

where a is the mean value of fitted xCO_2^{atm}, b is the mean annual increase (ppmv yr^{-1}), t is the number of days counted from January 1st, 2003, A_a and A_s are the amplitudes of the annual and seasonal harmonics (ppmv) and θ_a and θ_s are the annual and seasonal phases (Julian day), respectively.

After the curve was fitted, the residual standard deviation (σ_r) of the accepted data from the curve was calculated. Then if a rejected data point lay less than $3 \cdot \sigma_r$ from the curve, it was again incorporated in the accepted data set. The fit was iterated until no more measurements were flagged. The filtered data was weekly averaged and the definitive parameters of the seasonal curve were calculated for weekly data in each of the three selected zones (Fig. 2c; Table 1).

Finally, the quality of the atmospheric background level established by comparison the ship-board measurements to xCO_2^{atm} time series from land meteorological stations. Data were obtained from two nearby meteorological stations belonging to NOAA/ESRL Global Monitoring Division. Azores (Portugal, 38.77ºN, 27.37ºW) and Mace Head (Ireland, 53.55ºN, 9.15ºW) stations were chosen since the Bay of Biscay lies latitudinally between them. Monthly averaged xCO_2^{atm} from 1991 to 2002 of both reference points were fitted with equation 3.

3. RESULTS AND DISCUSSION

3.1 Seasonal variability of atmospheric xCO_2

The parameters obtained with the curve fitting in the three studied zones and the two NOAA meteorological stations are displayed in Table 1. The curves from the two NOAA stations were linearly interpolated from a new series at the latitude of the Bay of Biscay (45 ºN). These equations explain a high percentage of the total variance of the data at all sites (Table 1), with xCO_2^{atm} errors of ± 2, ± 1.5, ± 2.1, ± 1.7 and ± 1.3 ppmv in Galician offshore, Bay of Biscay, French offshore, Azores and Mace Head, respectively.

The atmospheric CO_2 trend rate (b, in Table 1) along the track during 2003-2004 (1.58 ± 0.10 ppmv yr^{-1}) was inferior to the mean value estimated in the Azores and Mace Head (1.76 ± 0.01 ppmv yr^{-1}) from 1991 to 2002. According to several studies, oscillations of the atmospheric CO_2 growth rate have a relationship with El Niño Southern Oscillation (ENSO) events (Bacastow 1976; Bacastow et al. 1980; Keeling et al. 1985; Thompson et al. 1986; Elliot et al. 1991). In spite of the small differences between our results and the NOAA observations, the growth rate at the studied sites is within the interannual fluctuation range of ± 0.2 reported by Conway et al. (1994).

The coupling of the two seasonal harmonics in the accepted data series display minimum and maximum values during August and late April, respectively. The xCO_2^{atm} maxima and minima are caused by photosynthetic activity in response to solar declination. Nevertheless, there is a three month delay between the maximum and minimum of irradiance and the corresponding extreme values of recorded xCO_2^{atm} (Fung et al. 1983, 1987; Keeling et al. 1976, 1996) that is clearly reflected in all of the fitted curves (Fig. 2c and Table 1). The summer minimum does not match perfectly due to a data gap of twenty days in August. The consequence is that the minimum xCO_2^{atm} presents a conspicuous uncertainty in both timing and magnitude. In contrast, the maximum in April is consistently reached throughout the whole area.

Towards mid-February, a second minimum stands out in the fitted curve (Fig. 2C). During this period, the wind pattern in the Bay of Biscay is dominated by south-westerly winds (Nogueira et al. 1997) and therefore with little influence from continental sources. The region is also characterized at this time of year by constituting an important area of CO_2 uptake (Follows et al. 1996) and for being the formation region of Eastern North Atlantic Central Water (Paillet & Mercier 1997).

With the purpose of assessing the xCO_2^{atm} depletion during wintertime due to the oceanic CO_2 uptake, a moving atmospheric mixing layer of 100 m (Stull, 1950) is considered over the Bay of Biscay for reported winter conditions. Stronger south-westerly winds and colder waters increase both the transfer velocity and the xCO_2 gradient facilitating the CO_2 exchange. Thus, the amount of xCO_2^{atm} that the Bay of Biscay could reduce in the estimated atmospheric column is around 2.50 ppmv. This result would explain the observed difference between the stable winter maximum shown by the curves from NOAA meteorological stations and the second winter minimum registered by the ship-board measurements. Ferrarese et al. (2002) suggests that seasonal xCO_2^{atm} anomalies between ocean and adjacent continental regions in the North Atlantic Ocean are produced by the seasonal surface temperature variation. Bousquet et al. (1996) also reported that air masses arriving from the ocean show depleted xCO_2^{atm} relative to all surrounding terrestrial stations within the North Atlantic basin. This conclusion is supported by the deepening of the motion of the winter minimum eastwards (Fig. 2c) in the dominant moving direction of air masses. Thus, the intensity of the winter minimum related to the latitudinal interpolation curve increase from the Galician offshore (1.7 ± 2 ppmv) to the French offshore (3.6 ± 2.1 ppmv), with a difference in the Bay of Biscay of 2.9 ± 1.5 ppmv. When looking at data, the relationship of xCO_2^{atm} anomalies ($_{DIF}CO_2^{atm}$) to the longitude (γ) from Azores for the 2003 winter, the rate found was:

$$_{DIF}CO_2^{atm} = 0.14 \cdot \gamma \qquad (r^2 = 0.91)$$

On the other hand, the peak-to-peak amplitude of the seasonal xCO_2^{atm} (Table 1) increases northward (Conway et al. 1988) from Azores (9.5 ppmv) to Ireland (13.5 ppmv) due to the significant release of anthropogenic CO_2 in northern regions (Rotty 1983) and the strong photosynthesis capacity of the boreal forest (Olson et al. 1983). The relationship found between the latitude (λ) from Azores to Mace Head and the peak-to-peak (p-to-p) amplitude is:

$$\text{p-to-p} = 0.27 \cdot \lambda - 1.02 \qquad (r^2 = 0.92)$$

3.2 Uncertainties in flux calculations

Apart from the errors derived from the fCO_2^{sw} measurements, air-sea fluxes are subject to other additional sources of error: atmospheric xCO_2, atmospheric pressure, wind speed and gas transfer coefficients.

In order to estimate the magnitude of the gas exchange in the Bay of Biscay the net CO_2 flux was calculated (Eq. 2) for the year 2003. The transfer velocity (k) was computed using remote wind speeds from QuikSCAT satellite observations following the Wanninkhof (1992) equation for short-term winds and subsequently weekly averaged. Net CO_2 exchange during the year is characterized by (Figure 3) an intense period of spring uptake related to biological activity (March – May, -9 ± 7 mmolC m^{-2} day^{-1}), a wintertime mixing (October – February, -6 ± 3 mmolC m^{-2} day^{-1}), and a summer period of wear gas exchange (June – September, -0.3 ± 0.8 mmolC m^{-2} day^{-1}). The summer increase of sea surface temperature leads the fCO_2^{sw} values close to those for the atmosphere minimizing the air-sea fCO_2 gradient. The annual mean CO_2 flux of -5 ± 5 mmolC m^{-2} day^{-1} confirms the role of this region as a CO_2 sink, as identified by Follows et al. (1996). This value lies within the flux range proposed by Borges (2005) for Bay of Biscay.

3.2.1 Atmospheric CO_2 molar fraction

Uncertainty arises from the choice of three options relative to weekly averaged values of xCO_2^{atm} measured in situ ($x_{ref}CO_2^{atm}$) in the Bay of Biscay:

a) the seasonal cycle fitted to ship-board measurements ($x_{FS}CO_2^{atm}$).

b) the latitudinal interpolation at 45ºN from the seasonal curves of NOAA stations (Azores (Portugal) – Mace Head (Ireland)) ($x_{NOAA}CO_2^{atm}$) (Kempe and Pegler 1991; Metzl et al. 1991; De Grandpre et al. 1998).

c) a constant value ($x_{CTE}CO_2^{atm}$), assuming the annual mean of $x_{NOAA}CO_2^{atm}$ and disregarding the xCO_2^{atm} variability (Stephens et al. 1995; Frankignoulle and Borges, 2001; Takahashi et al. 2002; Olsen et al. 2004).

In order to choose the best option for estimating in situ xCO_2^{atm} for the air-sea flux calculations, the error of CO_2 flux (ε_F) yielded by the xCO_2^{atm} differences is evaluated for 2003 according to Pérez et al. (2001):

$$\varepsilon_F = 0.24\ k\ S\ (x_{new}CO_2^{atm} - x_{ref}CO_2^{atm}) \qquad (4)$$

The reference value ($x_{ref}CO_2^{atm}$) is the weekly averaged values of in situ xCO_2^{atm} measured in the Bay of Biscay during 2003. The $x_{new}CO_2^{atm}$ (Figure 3) is the seasonal cycle fitted from on board measurements ($x_{FS}CO_2^{atm}$), latitudinal interpolation from NOAA stations ($x_{NOAA}CO_2^{atm}$) and a constant value ($x_{CTE}CO_2^{atm}$).

The use of $x_{FS}CO_2^{atm}$ relative to $x_{ref}CO_2^{atm}$ yields an averaged annual error of -0.02 ± 0.13 mmol m^{-2} day^{-1} (Fig. 4a). O course, the difference is practically negligible because $x_{FS}CO_2^{atm}$ was fitted from the weekly averages of in situ measurements ($x_{ref}CO_2^{atm}$). Nevertheless it is noteworthy that the maximum error is found during February (0.35 mmol m^{-2} day^{-1}) although the highest anomaly of xCO_2^{atm} is measured in July (2.9 ppmv).

Using any other xCO_2^{atm} alternatives, the CO_2 flux error notably increases. Thus, the bias increases to -0.2 ± 0.3 mmol m^{-2} day^{-1} with $x_{NOAA}CO_2^{atm}$ and -0.1 ± 0.4 mmol m^{-2}

day^{-1} with $x_{CTE}CO_2^{atm}$. In spite of the similarity between the flux uncertainties, it is important to underline the different nature of the errors. Thus, $x_{CTE}CO_2^{atm}$ yields a systematic error relative to the seasonal xCO_2^{atm} cycle. Positive anomalies (0.4 ± 0.3 mmol m^{-2} day^{-1}) are found during springtime (April – June) when the seasonal evolution reaches the highest xCO_2^{atm}. Conversely, negative errors are reached when $x_{CTE}CO_2^{atm}$ overestimates xCO_2^{atm}. Thus, during the lowest values of seasonal xCO_2^{atm} cycle (July – November), the flux is altered in -0.5 ± 0.2 mmol m^{-2} day^{-1} whereas during the winter minimum (January – February) the difference is -0.2 ± 0.2 mmol m^{-2} day^{-1}. In contrast, using the $x_{NOAA}CO_2^{atm}$ insignificant random errors are obtained except during wintertime. Negative anomalies of -0.5 ± 0.4 mmol m^{-2} day^{-1} are found from January to March when the largest discrepancy between NOAA meteorological station data and ship-board measurements (Fig. 3) occurs.

On the annual scale, choice of either $x_{CTE}CO_2^{atm}$ or $x_{NOAA}CO_2^{atm}$ would increase estimated the CO_2 uptake by 5% in the Bay of Biscay, with a net CO_2 flux of -5.2 mmolC m^{-2} day^{-1}. Even worse estimates in percentage terms could be obtained at particular times of year. For example, taking January to February, the use of $x_{NOAA}CO_2^{atm}$ instead of $x_{ref}CO_2^{atm}$ would accentuate the CO_2 sink role by 15%, i.e. -6 ± 2 to -7 ± 3 mmolC m^{-2} day^{-1}. Worse results could be obtained during periods of reduced gas exchange. Thus, from June to September, the use of $x_{CTE}CO_2^{atm}$ would increase the air-sea CO_2 difference, doubling the uptake capacity of the Bay of Biscay to -0.7 ± 0.8 mmolC m^{-2} day^{-1}. Conversely, the xCO_2^{atm} has a weaker effect on the net CO_2 flux during periods of intense exchange. Therefore, the most important error yielded by $x_{CTE}CO_2^{atm}$ during the springtime (0.4 ± 0.3 mmol m^{-2} day^{-1}), only represents 4% of the net CO_2 flux (-9 ± 7 mmol m^{-2} day^{-1}) from April to June.

Other parameters playing a critical role in the estimate of CO_2 fluxes can be obtained from different sources. The different estimates of atmospheric pressure and wind speed and different expressions for transfer velocity are studied by analyzing their influence on the calculated CO_2 exchange.

3.2.2 Atmospheric pressure

Sea level pressure is usually measured in situ (p_{IS}) although it can also be obtained from the NCEP/NCAR reanalysis project (p_{NCEP}) (Olsen et al., 2003; Lefèvre et al., 2004) or be taken as constant value (p_{CTE}). Weekly averages of the three options of atmospheric pressure were computed to convert the xCO_2^{atm} and fCO_2^{atm} (Eq. 1). The averaged discrepancy between p_{NCEP} and p_{IS} is -0.5 ± 0.8 kPa, with minimum differences found during summertime. The use of p_{NCEP} instead of p_{IS} results in an underestimation of fCO_2^{atm} of 2±2 μatm on annual scale. Therefore, the CO_2 uptake of the Bay of Biscay would be reduced by 0.3±0.2 $mmolC \cdot m^{-2} \cdot day^{-1}$ reaching maximum flux error values of 1.3 and -0.7 $mmolC \cdot m^{-2} \cdot day^{-1}$ during wintertime (Fig. 4b). Referenced to 1 atmosphere (101.325 kPa) as p_{CTE}, the annual mean of fCO_2^{atm} is increased in 0.2±0.4 μatm producing a slight change in the annual CO_2 flux of -0.1 ± 0.1 $mmolC \cdot m^{-2} \cdot day^{-1}$. The strongest differences are again found in January, namely, -1.5 and 1.1 $mmolC \cdot m^{-2} \cdot day^{-1}$.

3.2.3 Wind speed and k parameterizations

Nowadays the most frequent sources of wind speed data are the NCEP reanalysis model (W_{NCEP}) and the QuikSCAT satellite (W_{QS}). Wind speed at 10 m above the sea surface was obtained for 45ºN 6.5ºW from both sources. The weekly means of gas transfer velocity were computed using W_{NCEP} and W_{QS} according to the following parameterizations: Wanninkhof (1992) (k_W), Liss and Merlivat (1986) ($k_{L\&M}$) and Nightingale et al. (2000) (k_N). The W_{NCEP} is negatively biased (-1±1 $m \cdot s^{-1}$) compared to W_{QS} over the range 4 to 13 $m \cdot s^{-1}$. Consequently, the use of underestimated W_{NCEP} reduces by 14 ± 1% every transfer velocity and also the marked role of the Bay of Biscay as CO_2 sink. When computing CO_2 exchange with the two wind dataset (Fig. 4c), the flux estimates showed an annual mean difference of 1 ± 2 $mmolC \cdot m^{-2} \cdot day^{-1}$ with maximum disagreement occurring in weeks of intense CO_2 exchange, i.e., 4.7 $mmolC \cdot m^{-2} \cdot day^{-1}$ in November and -2.8 $mmolC \cdot m^{-2} \cdot day^{-1}$ in April.

Although the effect of the parameterizations of k in the air-sea CO_2 exchanges is well studied (Wanninkhof and McGilllis, 1999; Boutin et al., 2002; Olsen et al., 2005), the CO_2 flux is investigated here using W_{QS} and the different parametrizations of k, with $k_{L\&M}$ and k_N relative to k_W (Fig. 4c). A systematic and significant reduction of estimated gas exchange is obtained with $k_{L\&M}$ and k_N, reaching maximum flux errors of 6.9 and 3.1 $mmolC \cdot m^{-2} \cdot day^{-1}$ in April. The seasonal cycle of the two flux errors inversely reproduces the seasonal evolution of CO_2 flux (Fig. 3). Therefore, the influence of the k-bias depends directly on the module of wind speed and on the fCO_2 gradient. They both increase the effect of the transfer velocity, and its inaccuracies on the gas exchange computations. Thus, air-sea CO_2 exchange computed from the parameterization of Wanninkhof (1992) corresponds to an average of 139% of that from the formulation of Liss and Merlivat (1986) and 112% of that from Nightingale (2000), in agreement with the flux ratios proposed by Borges and Frankignoulle (2003).

3.2.4 Comparing the flux uncertainties

Results (Fig. 4) showed transfer velocity as the main source of flux uncertainty yielding systematic biases in agreement with conclusions of Wanninkhof and McGillis (1999), Boutin et al. (2002), Borges and Frankignoulle (2003). The contribution of the various sources of xCO_2^{atm}, sea level pressure and wind speed parameters to flux error were evaluated following Bevington and Robinson (1992). Deviations associated with these three parameters were computed for CO_2 exchange with k_W (Fig. 5).

The annual mean input of xCO_2^{atm}, sea level pressure and wind speed to the flux variance is of 17±23, 19±23 and 64±38% respectively. Once more the results show the strong sensitivity of CO_2 flux as well as $k_{L\&M}$ and k_N to the wind speed. Thus, wind speed would represent 59±37 and 60±38% of the flux uncertainties estimated with $k_{L\&M}$ and k_N, respectively. Wind speed has its most intense role during certain periods when significant disagreement between W_{NCEP} and W_{QS} coincides with intense gas exchange (99% in October 2003). In spite of having a smaller influence, xCO_2^{atm} becomes significant during summer, when it reaches 89% of the total error uncertainty. Atmospheric pressure influences a percentage of flux variance similar to xCO_2^{atm} and represents a similarly important term in flux error during summer (76%).

To quantify the relative contributions of each variable, the maximum error was estimated for the seasonal cycle (Fig. 5). So, an anomalous CO_2 exchange was computed using $x_{CTE}CO_2^{atm}$, p_{NCEP} , W_{NCEP} and $k_{L\&M}$ as opposed to the standard flux estimated with $x_{ref}CO_2^{atm}$, p_{IS} , W_{QS} and k_W. The mean maximum error on the annual scale is 2±2 $mmolC{\cdot}m^{-2}{\cdot}day^{-1}$. Therefore the CO_2 uptake capacity of the Bay of Biscay could be underestimated by 40% depending on the choice of the analyzed parameters. However, the flux difference could increase ~7 $mmolC{\cdot}m^{-2}{\cdot}day^{-1}$ during short periods in spring. The uncertainty also can be practically negligible or even reverse the regular sense of the anomaly to increase the sink behaviour of the region at 0.6 $mmolC{\cdot}m^{-2}{\cdot}day^{-1}$, as during summer. Therefore, the effect of xCO_2^{atm} and atmospheric pressure is often insignificant in spite of their important relative influence in the flux error. Thus, the maximum influence of xCO_2^{atm} (89%) reached in July represents only 0.01 mmolC·m^{-2}·day^{-1} whereas the atmospheric pressure yields no effects, even though it represents 76% of the maximum uncertainty in September. Nevertheless, wind speed becomes important during maximum uncertainties, increasing the critical influence in the estimate of CO_2 fluxes.

4. CONCLUSIONS

The ship-board xCO_2^{atm} measurements pose several difficulties resulting from ship's emissions and anthropogenic emissions from land. Therefore careful data processing is required to filter xCO_2^{atm} to identify the representative values of non-contaminated background conditions. Seasonal curves plus an annual trend are successfully used to fit the xCO_2^{atm} evolution in the Bay of Biscay during the years 2003–2004. The characteristics of estimated seasonal cycles are within the range shown by time series from land meteorological stations. However, a winter minimum of xCO_2^{atm} associated with an important oceanic CO_2 uptake and increasing eastward through the Bay of Biscay is not recorded by the meteorological stations.

The effect in CO_2 flux computations of the anomalies in xCO_2^{atm} is analyzed in the Bay of Biscay for the year 2003. Constant $x_{CTE}CO_2^{atm}$ yields systematically biased results that are compensated at long time scale whereas NOAA meteorological station $x_{NOAA}CO_2^{atm}$ produces correct xCO_2^{atm} compared to in situ observations at $x_{FS}CO_2^{atm}$ for the year except during winter, when the xCO_2^{atm} minimum is not reproduced. Using the $x_{CTE}CO_2^{atm}$ or $x_{NOAA}CO_2^{atm}$, the annual CO_2 exchange in the Bay of Biscay would be overestimated by ~5%. On the other hand, $x_{FS}CO_2^{atm}$ show optimum behaviour reporting an annual CO_2 flux of -5 mmolC·m^{-2}·day^{-1}. Providing in situ xCO_2^{atm} dataset is adequate to describe the background level of xCO_2^{atm}, the $x_{FS}CO_2^{atm}$ shows both several advantages and accurate results. Thus, the local seasonal xCO_2^{atm} cycle can be perfectly characterized throughout the year avoiding routine xCO_2^{atm} measurements.

Several available sources of sea level pressure, wind speed data and transfer velocity formulations were also evaluated. The atmospheric pressure can introduce a flux error of similar magnitude to that associated with the obtainable xCO_2^{atm}. Reanalysis pressure

p_{NCEP} underestimates CO_2 sink role in 0.3±0.2 mmolC·m^{-2}·day^{-1} whereas an assumed constant pressure p_{CTE} (1 atmosphere) does not affect flux computations. The use of W_{NCEP} compared to W_{QS} would typically represent an annual mean error of 14 ± 1% for each studied transfer velocity expression**,** which represent 72 ± 5% and 91 ± 4% for $k_{L\&M}$ and k_N, respectively, of CO_2 flux computed with k_W. Although wind speed and transfer velocity are the most important sources in flux uncertainty, their choice is of critical relevance during springtime. The role of xCO_2^{atm} and the atmospheric pressure also show seasonal variations that display a special importance during summertime. Therefore, in order to understand the real significance of xCO_2^{atm} results, it is fundamental to have knowledge of the source of parameters used in the calculations.

5. ACKNOWLEDGEMENTS

This work was developed and funded within the ECO project (MCyT REN2002-00503/MAR) and the European Commission (EU FP6 CARBOOCEAN Integrated Project, Contract no: 511176-2). "Diputation de Pontevedra" financed X.A. Padin with a predoctoral grant. We want to especially thank the captains and crews of RO-RO "L'Audace" and "Surprise", together with the management team of Suardiaz Company, for their hospitality and essential help throughout the two years. We also thank the NOAA/ESRL Global Monitoring Division for having provided atmospheric CO_2 flask data recorded at Azores and Mace Head and G. Navarro who kindly provided the remote sensing images processed in the Ocean Color Remote Sensing Service at ICMAN-CSIC. We thank Des Barton for revision of the English.

6. REFERENCES

Bacastow, R.B., 1976. Modulation of atmospheric carbon dioxide by the Southern Oscillation. Nature, 261:116–118.

Bacastow, R.B., Adams, J.A., Keeling, C.D., Moss, D.J., Whorf, T.P., Wong, C.S., 1980. Atmospheric Carbon dioxide, the Southern oscillation and the weak 1975 El Niño. Science, 210:66–68.

Bevington, P.R. and Robinson, D.K, 1992. Data reduction and error analysis for the physical sciences. Mc. Graw-Hill, New York.

Boden, T.A., Sepansky, R.J. and Stoss, F.W., 1991. A Compendium of Data on Global Change, Carbon Dioxide Information Analysis Center. Trends ´91, Tennessee.

Boehm, A.B. and Grant, S.B., 1998. Influence of coagulation, sedimentation, and grazing by zooplankton on phytoplankton aggregate distributions in aquatic systems. Journal of Geophysical Research, 103(C8):15601–15612.

Borges, A.V. and Frankignoulle, M., 2002. Distribution and air-water exchange of carbon dioxide in the Scheldt plume off the Belgian coast. Biogeochemistry, 59:41–67.

Borges, A.V. and Frankignoulle, M., 2003. Distribution of surface carbon dioxide and air-sea exchange in the English Channel and adjacent areas. Journal of Geophysical Research, 108(C5), doi: 10.1029/2000JC000571.

Borges, A.V., 2005. Do we have enough pieces of the jigsaw to integrate CO_2 fluxes in the coastal ocean? Estuaries, 28:3–27.

Bousquet, P., Gaudry, A., Ciais, P., Kazan, V., Monfray, P., Simmonds, P.G., Jennings, S.G. and O'Connor, T.C., 1996. Atmospheric CO_2 concentration variations recorded at Mace Head, Ireland, from 1992 to 1994. Physics and Chemistry of the Earth, 21(5-6):477–481.

Boutin, J., Etcheto, J., Merlivat, L. and Rangama, Y., 2002. Influence of gas exchange coefficient parameterization on seasonal and regional variability of CO_2 air-sea fluxes. Geophysical Research Letters, 29, doi: 10.1029/2001GL013872.

Conway, T.J., Tans, P., Waterman, L.S., Thoning, K.W., Masarie, K.A. and Gammon, R.H., 1988. Atmospheric carbon dioxide measurements in the remote global troposphere. Tellus, 40(B):81–115.

Conway, T.J., Tans, P.P., Waterman, L.S., Thoning, K.W., Kitzis, D.R., Masarie, A. and Zhang, N., 1994. Evidence for interannual variability of the carbon cycle from the national oceanic and atmospheric administration/climate monitoring and diagnostics laboratory global air sampling network. Journal of Geophysical Research, 99:22831–22855.

Cooper, D.J., Watson, A.J. and Ling, R.D., 1998. Variation of p CO_2 along a North Atlantic shipping route (U.K. to Caribbean): A year of automated observations. Marine Chemistry, 60:147–164.

DeGrandpre, M.D., Hammar, T.R. and Wirick, C.D., 1998. Short-term pCO_2 and O_2 dynamics in California coastal waters. Deep Sea Research II, 45:1557–1575.

DeGrandpre, M.D., Olbu, G.J., Beatty, C.M. and Hammar, T.R., 2002. Air-sea CO_2 fluxes on the US Middle Atlantic Bight. Deep Sea Research II, 49:4355–4367.

DOE, 1994. Handbook of methods for the analysis of various parameters of carbon dioxide in seawater; version 2. In: Dickson, A.G., Goyet, C. (Eds.), ORNL/CDIAC-74.

Elliot, W.P., Angell, J.K. and Thoning, K.W., 1991. Relation of atmospheric CO_2 to tropical sea and air temperatures and precipitation. Tellus, 43(B):144–155.

Ferrarese, S., Longhetto, A., Cassardo, C., Apadula, F., Bertoni, D., Giraud, C. and Gotti, A., 2002. A study of seasonal and yearly modulation of carbon dioxide sources and sinks, with a particular attention to the Boreal Atlantic Ocean. Atmospheric Environment, 36:5517–5526.

Follows, M.J., Williams, R.G. and Marshall, J.C., 1996. The solubility pump of carbon in the subtropical gyre of the North Atlantic. Journal of Marine Research, 54:605–630.

Frankignoulle, M. and Borges, A.V., 2001. European continental shelf as a significant sink for atmospheric carbon dioxide. Global Biogeochemical Cycles, 15(3):569–576.

Fung, I.Y., Prentice, K., Matthews, E., Lerner, J. and Russell, G., 1983. Three-dimensional tracer model study of atmospheric CO_2: response to seasonal exchanges with the terrestrial biosphere. Journal of Geophysical Research, 88:1281–1294.

Fung, I.Y., Tucker, C.J. and Prentice, K.C., 1987. Application of advanced very high resolution radiometer vegetation index to study atmosphere-biosphere exchange of CO_2. Journal of Geophysical Research, 92:2999–3015.

Gillete, D.A., Komhyr, W.D., Waterman, L.S., Steele, L.P. and Gammon, R.H., 1987. The NOAA/GMCC continuous CO_2 record at the South Pole, 1975-1982. Journal of Geophysical Research, 92:4231–4240.

Hood, E.M., Merlivat, L. and Johannessen, T., 1999. Variations of f CO_2 and air-sea flux of CO_2 in the Greenland sea gyre using high-frequency time series data from CARIOCA drift buoys. Journal of Geophysical Research, 104(C9):20571–20583.

Jabaud-Jan, A., Metzl, N., Brunet, C., Poisson, A. and Schauer, B., 2004. Interannual variability of the carbon dioxide system in the southern Indian Ocean (20ºS-60ºS): The impact of a warm anomaly in austral summer 1998. Global Biogeochemical Cycles 18 (GB1042), doi: 10.1029/2002GB002017.

Kalnay, E., Kanamitsu, M., Kistler, R., Collins, W., Deaven, D., Gandin, L., Iredell, M., Saha, S., White, G., Woollen, J., Zhu, Y., Chelliah, M., Ebisuzaki, W., Higgins, W., Janowlak, J., Mo, K.C., Ropelewski, C., Wang, J., Leetmaa, A., Reynolds, R., Jenne, R. and Joseph, D., 1996. The NCEP/NCAR Reanalysis Project. Bulletin American Meteorological Society 77, 437–471.

Keeling, C.D., Bacastow, R.B., Bainbridge, A.E., Ekdahl Jr, C.A., Guenther, P.R., Waterman, L.S. and Chin, J.F.S., 1976. Atmospheric carbon dioxide variations at Mauna Loa Observatory, Hawaii. Tellus, 28:538–551.

Keeling, C.D., Whorf, T.P., Wong, C.S. and Bellagay, R.D., 1985. The concentration of atmospheric carbon dioxide at ocean weather station p from 1969 to 1981. Journal of Geophysical Research, 90(D6):10511–10528.

Keeling, R.F. and Shert, S.R., 1992. Seasonal and interannual variations in atmospheric oxygen and implications for the global carbon cycle. Nature, 358:723–727.

Keeling, C.D., Chin, J.F.S. and Whorf, T.P., 1996. Increased activity of northern vegetation inferred from atmospheric CO_2 measurements. Nature, 382:146–149.

Kempe, S. and Pegler, K., 1991. Sinks and sources of CO_2 in coastal seas: the North Sea. Tellus, 43(B):224–235.

Komhyr, W.D., Gammon, R.H., Harris, T.B., Waterman, L.S., Conway, T.J., Taylor, W.R. and Thoning, K.W., 1985. Global atmospheric CO_2 distribution and variations from 1968-1982 NOAA/GMCC CO_2 flask sample data. Journal of Geophysical Research, 90(D3):5567–5596.

Lefèvre, N., Moore, G., Aiken, J., Watson, A., Cooper, D. and Ling, R., 1998. Variability of CO_2 in the tropical Atlantic in 1995. Journal of Geophysical Research, 103(C3):5623–5634.

Lefèvre, N., Watson, A.J., Cooper, D.J., Weiss, R.F., Takahashi, T. and Sutherland, S.C., 1999. Assessing the seasonality of the oceanic sink for CO_2 in the Northern Hemisphere. Global Biogeochemical Cycles, 13(2):273–286.

Lefèvre, N. and Moore, G.F., 2000. Distribution of the CO_2 partial pressure along an Atlantic Meridional transect. Progress in Oceanography, 45:401–413.

Lefèvre, N., Olsen, A., Ríos, A., Pérez, F.F., Johannensen, T., 2004. A decrease in the sink for atmospheric CO2 in the North Atlantic. Geophysical Research Letters, 31, doi:2003GL018957.

Liss, P.S. and Merlivat, L., 1986. Air–sea gas exchange rates: introduction and synthesis. In: The role of air–sea exchange in geochemical cycling. Ed. Buat-Ménard, P., Norwell.

Metzl, N., Beauverger, C., Brunet, C., Goyet, C. and Poisson, A., 1991. Surface water carbon dioxide in the southwest Indian sector of the Southern Ocean: a highly variable CO_2 source/sink region in summer. Marine Chemistry, 35:85–95.

Nightingale, P.D., Liss, P.D. and Schlosser P., 2000. Measurements of air-sea gas transfer during an open ocean algal bloom. Geophysical Research Letters, 27:2117–2120.

Nogueira, E., Pérez, F.F. and Ríos, A.F., 1997. Seasonal patterns and long-term trends in an estuarine upwelling ecosystem (Ría de Vigo, NW Spain). Estuarine, Coastal and Shelf Science, 44:285–300.

Olsen, A., Bellerby, R.G.J., Johannsessen, T., Omar, A.M. and Skjelvan, I., 2003. Interannual variability in the wintertime air–sea flux of carbon dioxide in the northern Norht Atlantic. Deep Sea Research, 50:1323–1338.

Olsen, A., Triñanes, J.A. and Wanninkhof, R., 2004. Sea–air flux of CO_2 in the Caribbean Sea estimated using in situ and remote sensing data. Remote Sensing of Environment, 89(3):309–325.

Olsen, A., Wanninkhof, R., Triñanes, J.A. and Johannessen, T., 2005. The effect of wind speed products and wind speed-gas exchange relationships on interannual variability of the air–sea CO_2 gas transfer velocity. Tellus, 57B:95–106.

Olson, R.J., Frankel, S.L. and Chisholm, S.W., 1983. An inexpensive flow cytometer for the analysis of fluorescence signals in phytoplankton: chlorophyll and DNA distributions. Journal of Experimental Marine Biology and Ecology, 68:129–144.

Paillet, J. and Mercier, H. 1997. An inverse model of the eastern North Atlantic general circulation and thermocline ventilation. Deep-Sea Research I, 44(8):1293–1328.

Pérez, F.F., Gago, J., Alvarez, M. and Ríos, A.F., 2001. Temporal variability of atmospheric CO_2 of the Spanish Atlantic coast. Oceanologica Acta, 24:11–18.

Peterson, J.T., Komhyr, W.D., Waterman, L.S., Gammon, R.H., Thoning, K.W. and Conway, T.J., 1986. Atmospheric CO_2 variations at Barrow, Alaska, 1973-1982. Journal of Atmospheric Chemistry, 4:491–510.

Rotty, R.M., 1983. Distribution of and changes in industrial carbon dioxide production. Journal of Geophysical Research, 88:1301–1308.

Stephens, M.P., Samuels, G., Olson, D.B., Fine, R.A. and Takahashi, T., 1995. Sea-air flux of CO_2 in the north Pacific using shipboard and satellite data. Journal of Geophysical Research, 100(C7):13571–13583.

Stull, R.B., 1950. An introduction to Boundary Layer Meteorology. Kluwer Academic Publishers, Dordrecht.

Takahashi, T., Olafsson, J., Goddard, J.G., Chipman, D.W., Sutherland, S.C., 1993. Seasonal variation of CO_2 and nutrients in the high-latitude surface oceans: a comparative study. Global Biogeochemical Cycles, 7(4):843–878.

Takashashi, T., Sutherland, S.C., Sweeny, C., Poisson, A., Metzl, N., Tilbrook, B., Bates, N., Wanninkhof, R., Feely, R.A., Sabine, C., Olafsson, J., Nojiri, Y., 2002. Global Sea-Air CO2 flux based on climatological surface ocena pCO_2 and seasonal biological and temperature effects. Deep Sea Research, 49:1601–1622.

Thompson, M.L., Enting, I.G. Pearman, G.I. and Hyson, P., 1986. Interannual variations of atmospheric CO_2 concentration. Journal of Atmospheric Chemistry, 4:125–155.

Thoning, K.W., Tans, P.P. and Komhyr, W.D., 1989. Atmospheric carbon dioxide at Mauna Loa Observatory, 2, Analysis of the NOAA GMCC data, 1974-1985. Journal of Geophysical Research, 94:8549–8565.

Wanninkhof, R., 1992. Relationship between wind speed and gas exchange over the ocean. Journal of Geophysical Research, 97(C5):7373–7382.

Wanninkhof, R., McGillis, W.R., 1999. A cubic relationship between air-sea CO2 exchange and wind speed. Geophysical Reseach Letters, 26(13):1889–1892.

Weiss, R.F., 1974. Carbon dioxide in water and seawater: the solubility of non-ideal gas. Marine Chemistry, 2:203–215.

Figure captions

Figure 1: Map of the study site showing the typical route covered by the ships of opportunity between Vigo (Spain)-Saint Nazaire (France), depicted as black solid line. The partial tracks averaged to compare the study zones of Galician offshore, Bay of Biscay and French offshore are represented by a grey line and circles that indicate the backtrajectory of possible air masses, continental (black sector) or oceanic (white sector). Histograms display the percentage of backtrajectory, both oceanic (white bars) and continental (black bars), of each studied zone from 2003 to 2004: raw data and selected data.

Figure 2: Atmospheric molar fraction of CO_2 data measured in Bay of Biscay and the selection data process: a) all available measurements in Bay of Biscay are displayed; b) the data selected by the first criterion (see text) are plotted (black circles) along with the filtered data (white circles); c) the smoothed curves obtained, using the cited selection criteria, for Galician offshore (dash line), Bay of Biscay (black line), French offshore (grey line) and the latitudinally interpolated curve (dash grey line) from NOAA stations.

Figure 3: Weekly averages of measured xCO_2^{atm} in the Bay of Biscay ($x_{ref}CO_2^{atm}$; open circles) are shown from January to December 2003 with the different xCO_2^{atm} alternatives: seasonal curve fitted from ship-board measurements ($x_{FS}CO_2^{atm}$; black line), latitudinally interpolated curve from NOAA data ($x_{NOAA}CO_2^{atm}$; grey line) and the averaged value ($x_{CTE}CO_2^{atm}$; dashed line). Weekly averages of air–sea CO_2 flux ($mmol \cdot m^{-2} \cdot day^{-1}$, grey circles) in the Bay of Biscay computed with $x_{ref}CO_2^{atm}$ throughout 2003 are also included.

Figure 4: Errors of the CO_2 flux (ε_F, $mmol \cdot m^{-2} \cdot day^{-1}$) in the Bay of Biscay associated with different sources of: a) three different atmospheric CO_2 molar fractions relative to weekly averages of measured xCO_2^{atm}: seasonal curve fitted from ship-board measurements ($x_{FS}CO_2^{atm}$; black line and open circles), latitudinally interpolated curve from NOAA data ($x_{NOAA}CO_2^{atm}$; grey line) and averaged values ($x_{CTE}CO_2^{atm}$; dashed line and black circles). b) Sea level pressure relative to in situ atmospheric pressure: sea level pressure from the NCEP/NCAR reanalysis project (p_{NCEP}; black line) and constant value (p_{CTE}; grey line). c) Wind speed from NCEP reanalysis model (W_{NCEP}; black

circles and dashed line) and transfer velocity relative to Wanninkhof (1992): Nightingale (2000) (k_N; grey line) and Liss and Merlivat (1986) ($k_{L\&M}$; black line).

Figure 5: Percentage of air–sea CO_2 flux variance associated with the largest discrepancies between of xCO_2^{atm} ($x_{ref}CO_2^{atm}$ and $x_{CTE}CO_2^{atm}$, black bar), sea level pressure (p_{IS} and p_{NCEP}, white bar) and wind speed (W_{QS} and W_{NCEP}, grey bar) computed using Wanninkhof (1992). Maximum flux error (ε_F, mmol·m^{-2}·day^{-1}) estimated as the difference between a standard ($x_{ref}CO_2^{atm}$, p_{IS}, W_{QS} and k_W) and anomalous ($x_{CTE}CO_2^{atm}$, p_{NCEP}, W_{NCEP} and $k_{L\&M}$) gas exchange estimate for year 2003 in the Bay of Biscay (black line and white circle).

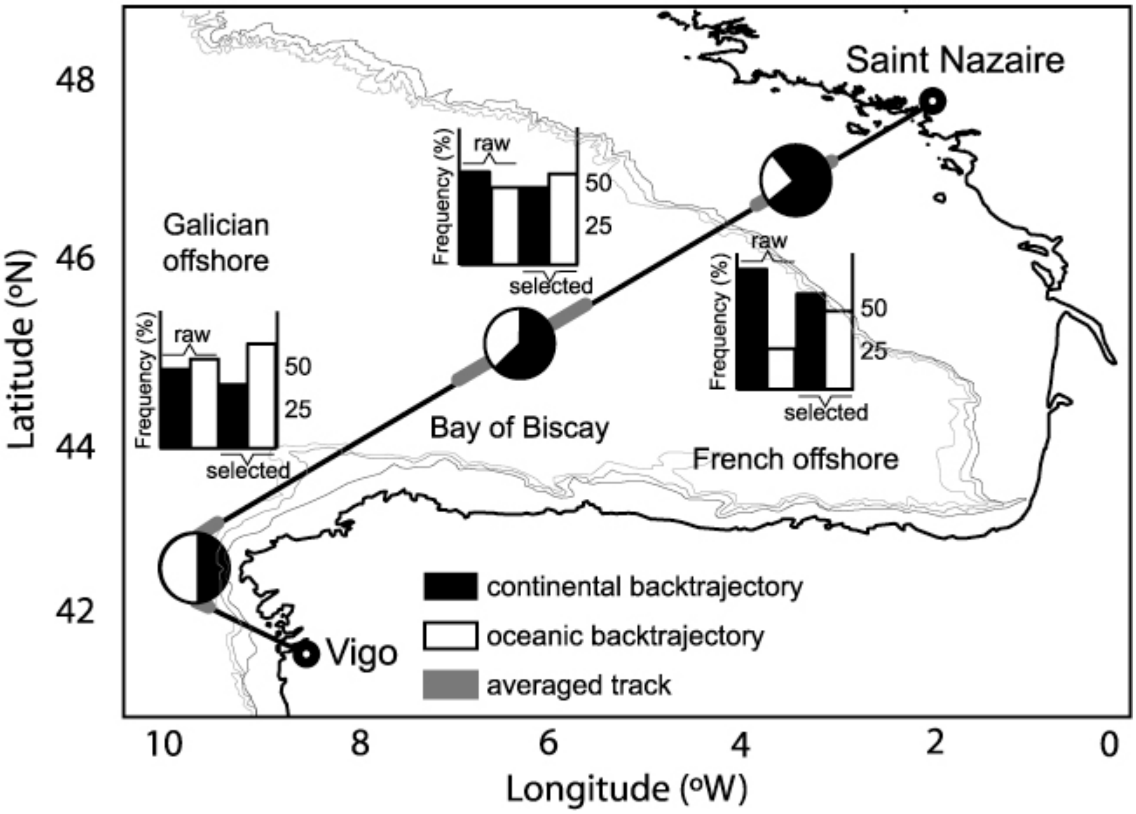

Saint Nazaire
Galician offshore
Bay of Biscay
French offshore
Vigo
raw
selected
Frequency (%)
50
25
continental backtrajectory
oceanic backtrajectory
averaged track
Latitude (°N)
48
46
44
42
Longitude (°W)
10
8
6
4
2
0

Figure 1

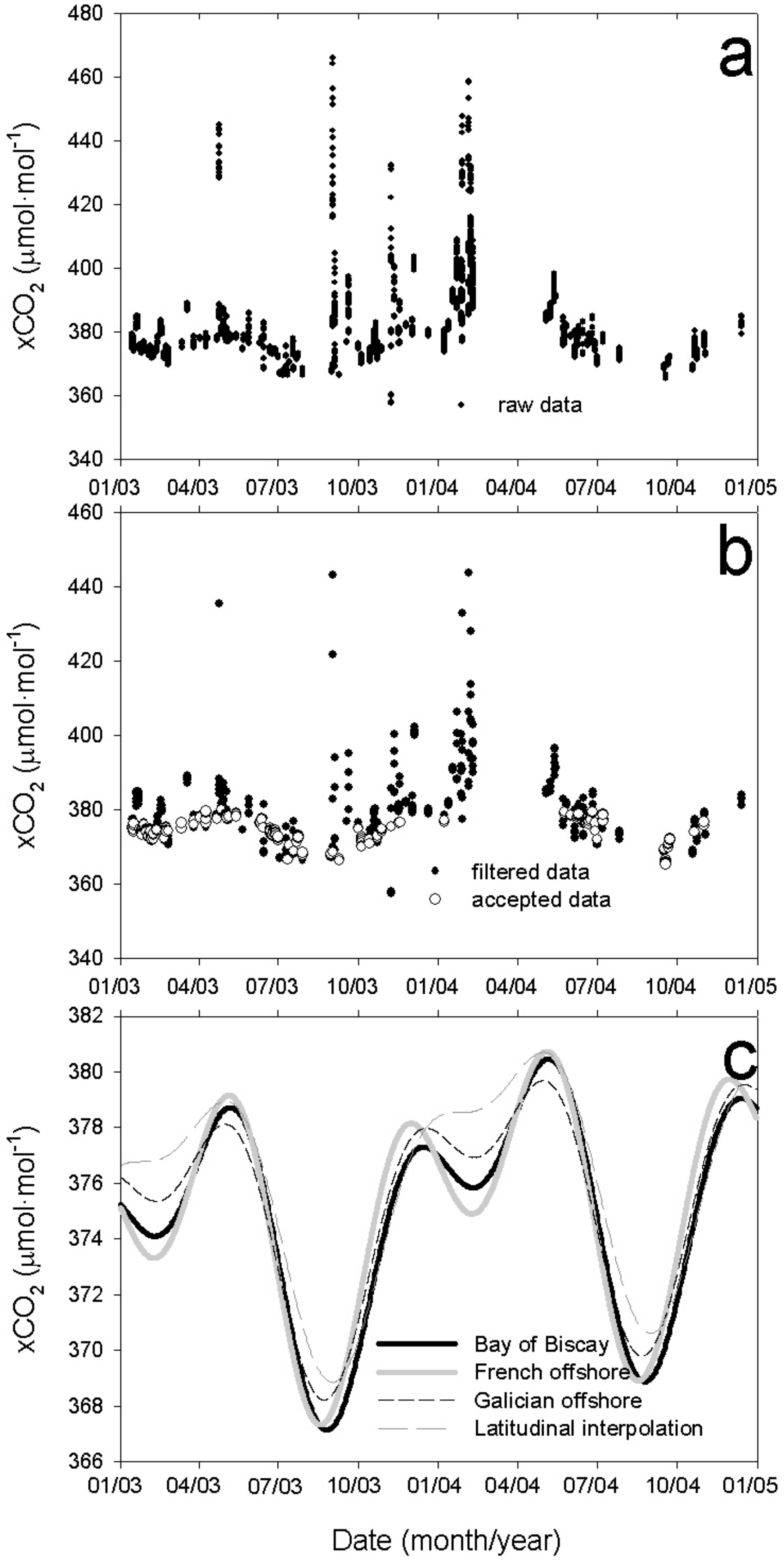
a
raw data
b
filtered data
accepted data
c
Bay of Biscay
French offshore
Galician offshore
Latitudinal interpolation
xCO2 (µmol·mol-1)
01/03
04/03
07/03
10/03
01/04
04/04
07/04
10/04
01/05
Date (month/year)

Figure 2

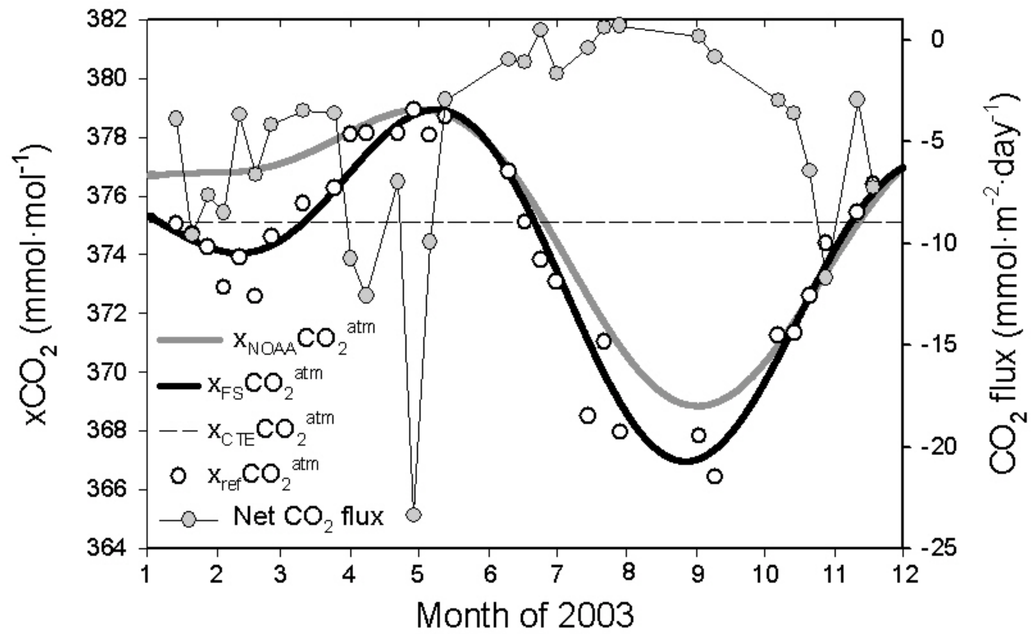

382
380
378
376
374
372
370
368
366
364
1
2
3
4
5
6
7
8
9
10
11
12
0
-5
-10
-15
-20
-25
xCO2 (mmol·mol-1)
CO2 flux (mmol·m-2·day-1)
Month of 2003
xNOAACO2atm
xFSCO2atm
xCTECO2atm
xrefCO2atm
Net CO2 flux

Figure 3

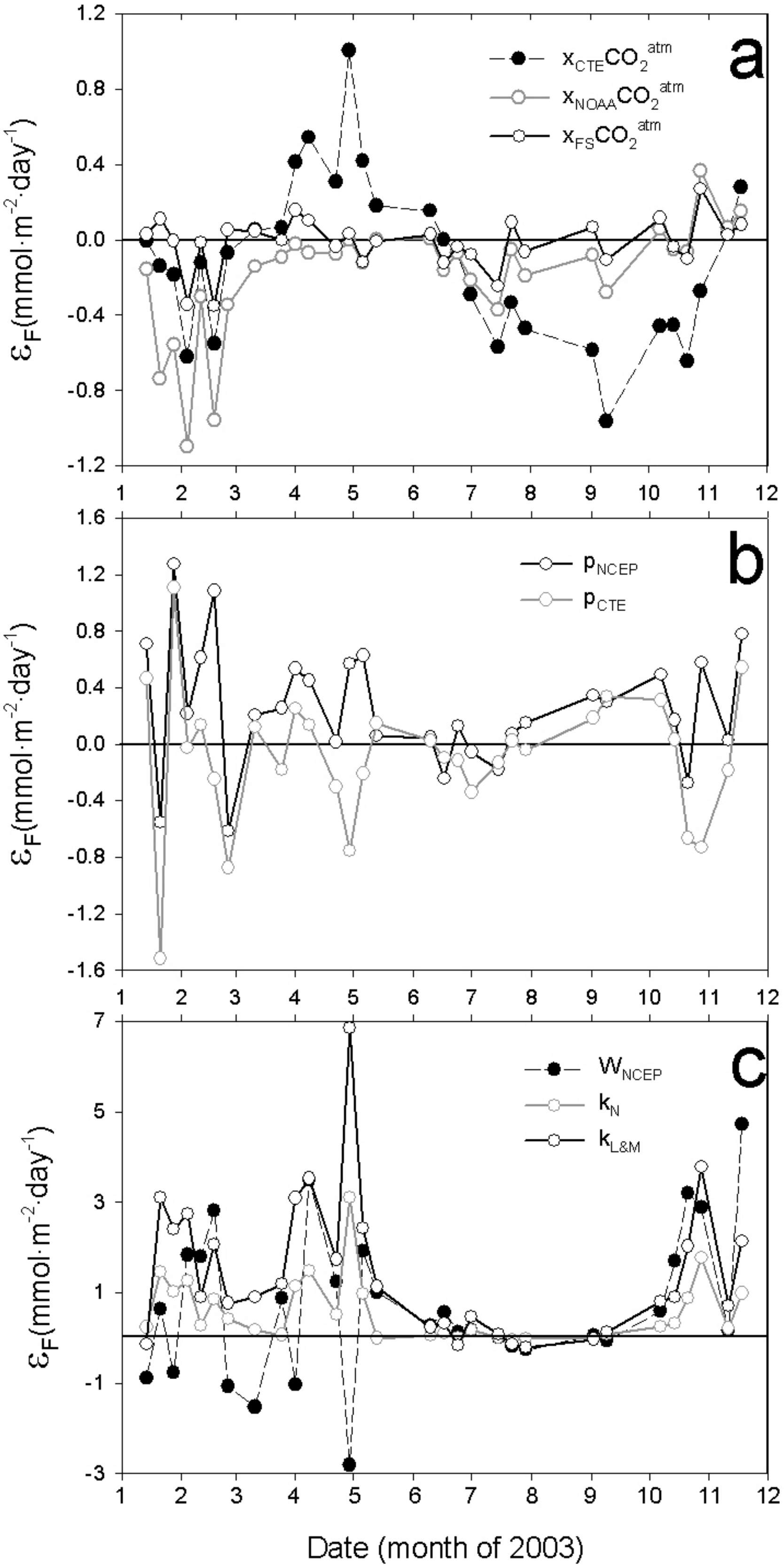

a
$x_{CTE}CO_2^{atm}$
$x_{NOAA}CO_2^{atm}$
$x_{FS}CO_2^{atm}$
b
p_{NCEP}
p_{CTE}
c
W_{NCEP}
k_N
$k_{L\&M}$
ε_F(mmol·m^{-2}·day^{-1})
Date (month of 2003)

Figure 4

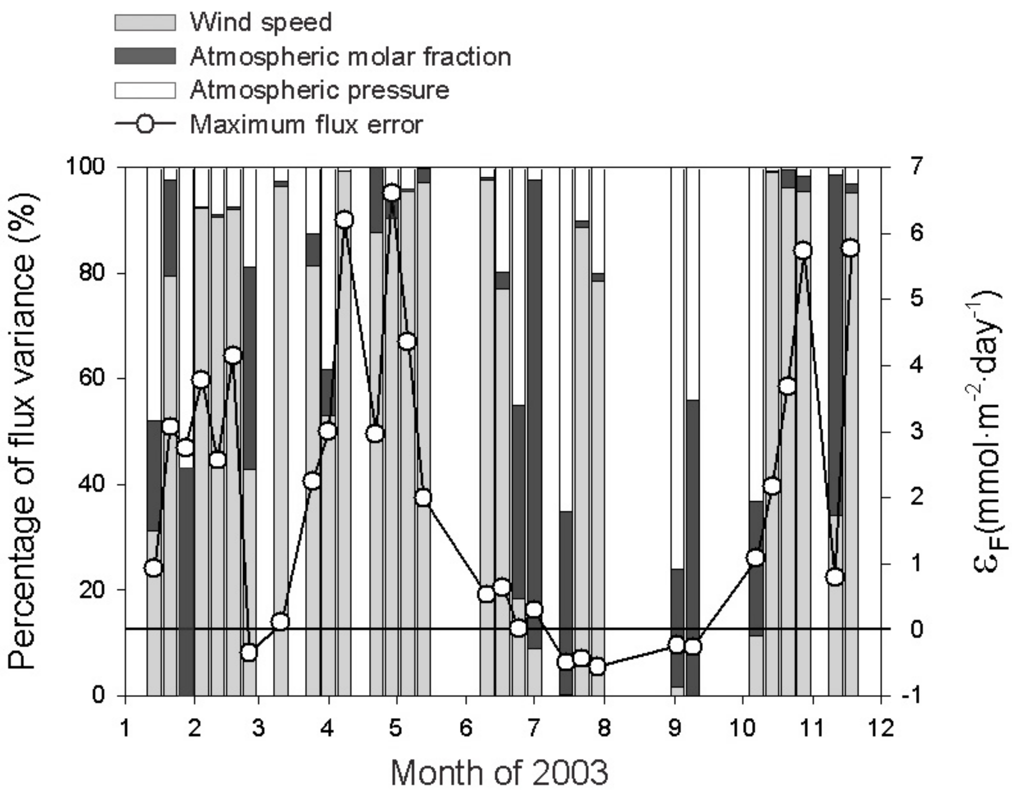
Wind speed
Atmospheric molar fraction
Atmospheric pressure
Maximum flux error
Percentage of flux variance (%)
ε_F(mmol·m^{-2}·day^{-1})
Month of 2003
100
80
60
40
20
0
7
6
5
4
3
2
1
0
-1
1
2
3
4
5
6
7
8
9
10
11
12

Figure 5

Table 1: Coefficients of seasonal curves according to Equation 3 in three regions of the Bay of Biscay and two NOAA meteorological stations. Regression coefficients (r^2), number of fitted values (n), amplitude of seasonal cycle (p-to-p) and the latitudinally interpolated seasonal curve from NOAA stations for the Bay of Biscay (45 ºN) are also included.

AREA	**a***	**b**	**A_a**	**θ_a**	**A_s**	**θ_s**	**r^2**	**n**	**p-to-p**
Azores	*374.1*	*1.76*	*-3.80*	*170*	*1.57*	*-77*	*0.96*	139	*9.5*
Mace Head	*374.1*	*1.76*	*-6.10*	*155*	*2.63*	*-80*	*0.97*	139	*13.2*
Lat. Interpolation	374.2	1.76	-4.65	163	1.97	-78	_	_	10.1
Galician offshore	373.7	1.57	-4.03	151	2.51	-96	0.87	52	9.9
Bay of Biscay	373.2	1.57	-4.22	163	3.23	-84	0.98	52	11.2
French offshore	373.5	1.59	-3.55	153	3.74	-91	0.91	52	11.9

* referred to 1 January 2003